Supporting Information (SI) for

Efficient Methanolysis of PET toward High-Purity DMT via Homo-Heterogeneous Mn^{2+}/Mn_2O_3 Synergistic Catalysis

Lei Yang[a], Jiacheng Gao[a], Min Su[b], Li Yuan[a], Yuan Wang[a], Dajun Wang[b], Heng Zheng[b], Shaojun Yuan[a] and Like Ouyang[a]*

[a] School of Chemical Engineering, Sichuan University, Chengdu, 610065, China

[b] State Key Laboratory of Porous Materials for Separation and Conversion, Southwest Institute of Chemical Co., Ltd, Chengdu, 610065, China

* Corresponding E-mail: Like.ouyang@scu.edu.cn (L.K. Ouyang)

Number of Pages:59

Number of Figures: 28

Number of Tables: 20

Contents

Part 1 Supplementary Figures

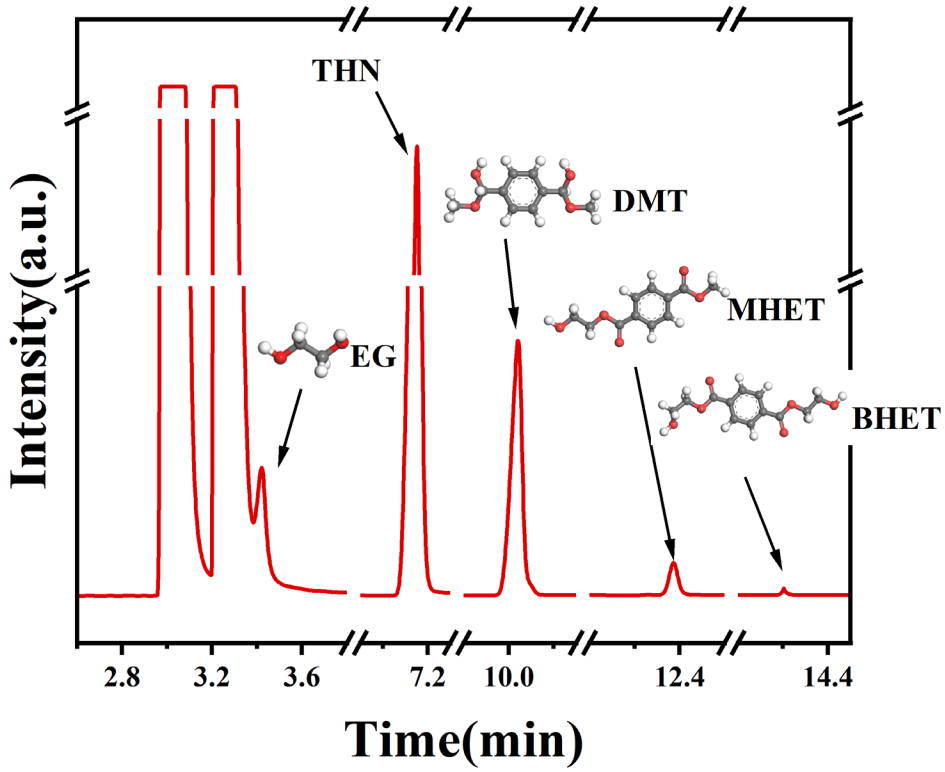

Figure. S1. Chromatographic peak sequence of products and internal standard.

Note： The liquid products were qualitatively identified and quantitatively analyzed using a Gas Chromatograph (GC2060). A micro-syringe was employed for direct liquid injection into the injector port. Argon served as the carrier gas. Separation was achieved using an HP-5 capillary column (30 m × 0.32 mm × 0.25 μm, Agilent) with a temperature-programmed method, and the signals were detected by a flame ionization detector (FID). The instrumental parameters were set as follows: both the injector port and the detector were maintained at 300 ℃. The oven temperature was programmed starting at 100 ℃, then ramped at a rate of 20 ℃/min to 300 ℃, and finally held at 300 ℃ for 12 minutes. The injection volume was 1 μL, the internal standard substance is tetrahydronaphthalene.

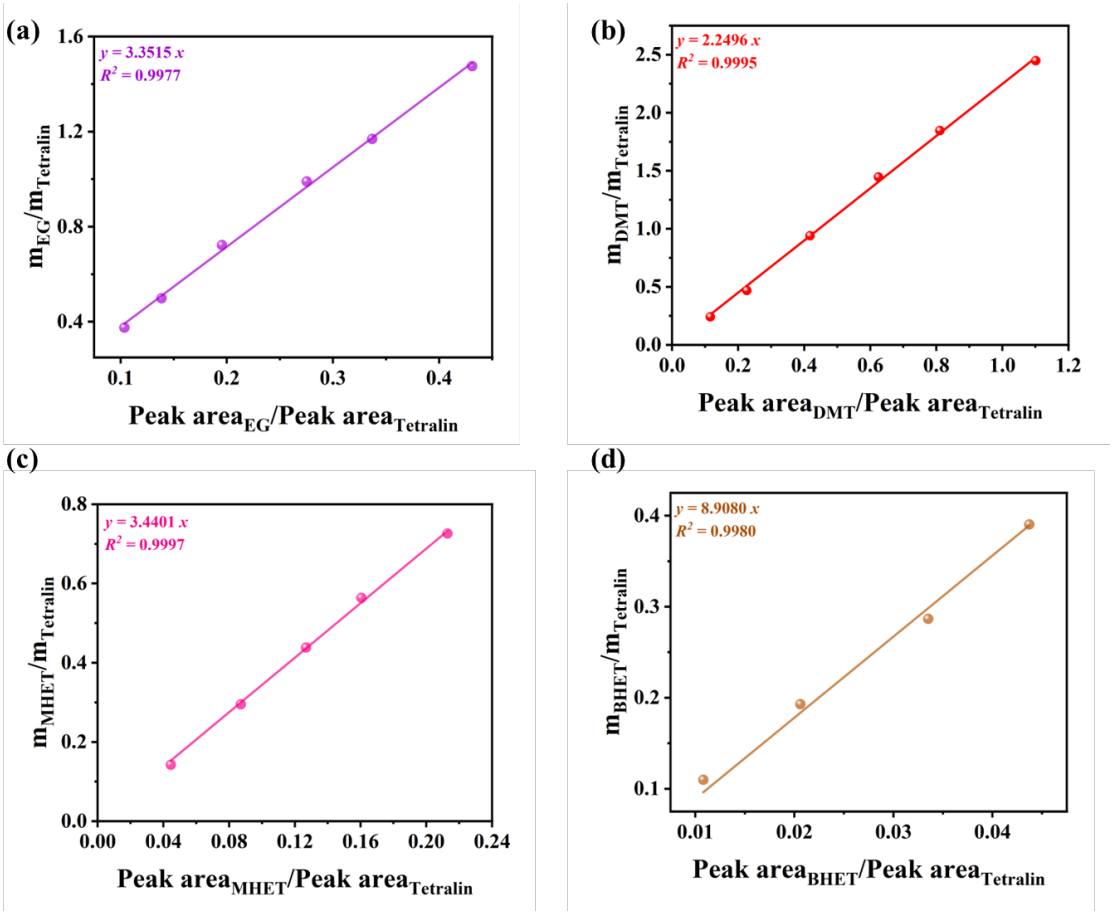

Figure. S2. Chromatographic internal standard curve for (a) EG, (b) DMT, (c) MHET and (d) BHET, using tetralin as the internal standard.

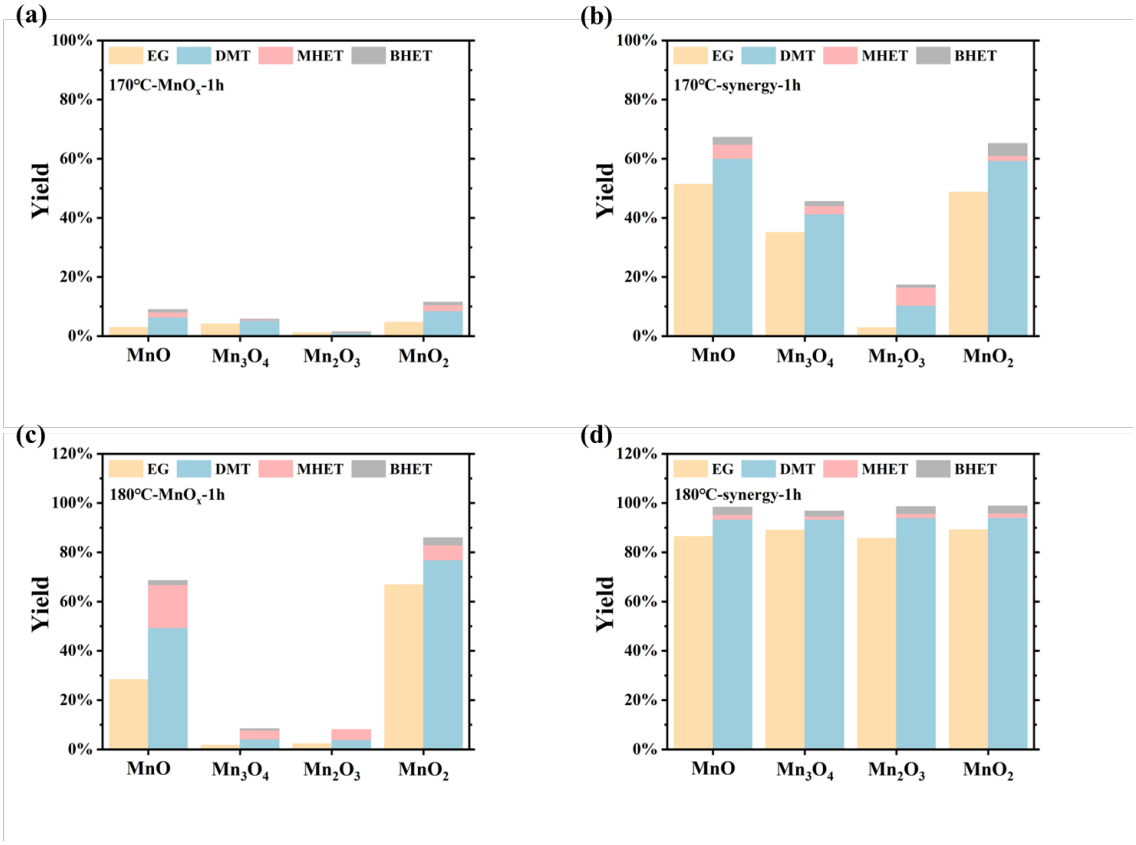

Figure. S3. Yield of products by single oxide and synergistic system at 170 ℃ (a, b) and 180 ℃ (c, d), calculated by internal standard method.

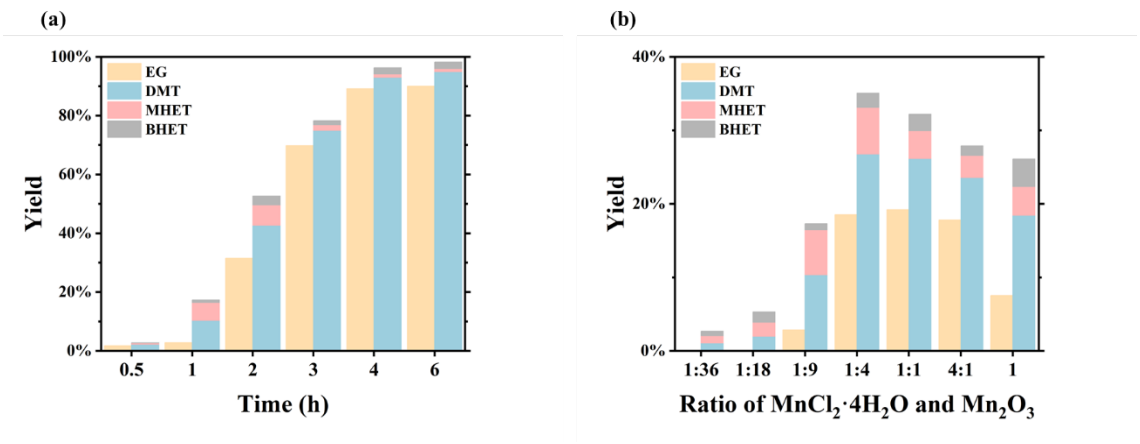

Figure. S4. Yield of products at (a) different times (170 ℃-10wt% catalyst) and (b) mass ratios of $MnCl_2·4H_2O$ and Mn_2O_3 (170 ℃-10wt% catalyst-1 h), calculated by internal standard method.

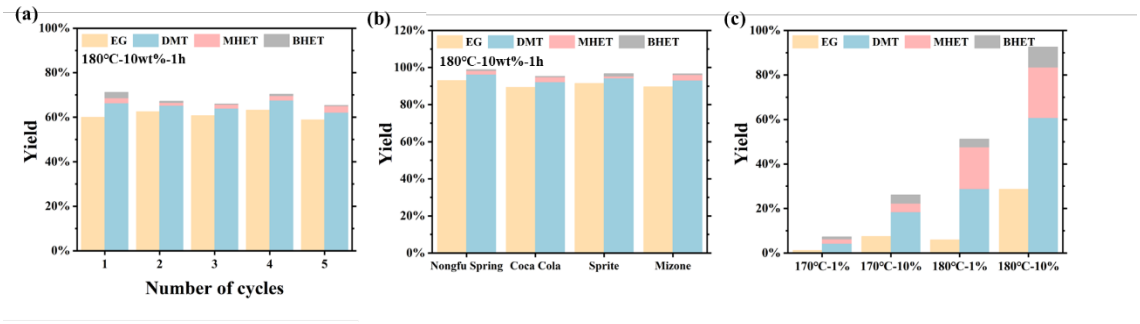

Figure. S5. (a) product yields over repeated catalyst recycling, (b) yield of products from different commercial plastics, (c) yield of products under different Mn^{2+} contents at 170 ℃ and 180 ℃ for 1 hour, calculated by internal standard method.

Note: The total catalyst mass is 10% ($MnCl_2 \cdot 4H_2O$: Mn_2O_3=1:9) of the PET mass for Fig.a and b. In each recycling cycles, fresh 50% mass fraction of homogeneous and heterogeneous catalysts are added. The homogeneous catalyst is obtained by freezing the methanol solution from the previous reaction and separating the solid phase products to obtain a methanol solution containing manganese ions. The heterogeneous catalyst is obtained by dissolving the products in chloroform and centrifuging the solution to dry it.

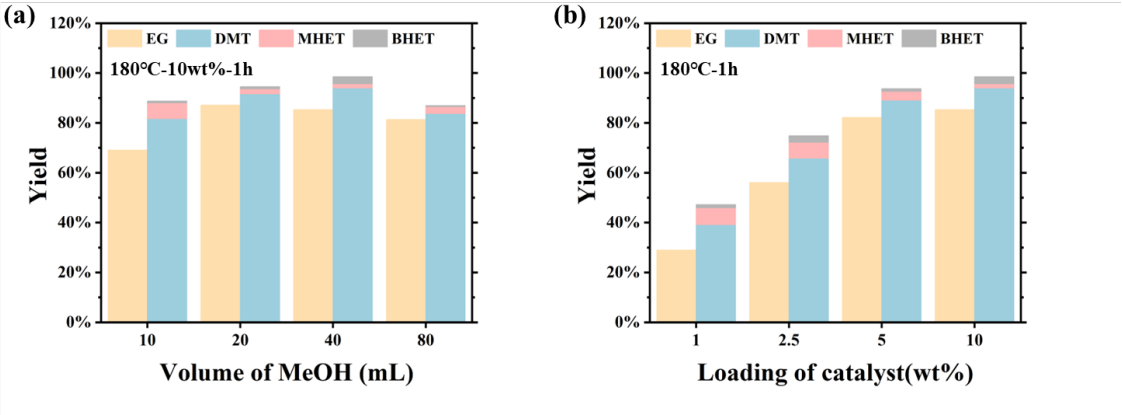

Figure. S6. (a) Conversion of PET and yield of products with different volumes of methanol at 180 ℃ for 1 hour. (b) conversion of PET and yield of products with different loading of catalyst at 180 ℃ for 1 hour.

Note: For Fig. S6a, the total catalyst mass is 10% ($MnCl_2 \cdot 4H_2O$: Mn_2O_3=1:9) of the PET mass, due to equipment limitations, in actual reactions, the 10 mL methanol group experiment used 20 ml methanol and 2 g PET, while the 80 ml methanol group experiment used 40 ml methanol and 0.5g PET which leads to a decrease in its PET conversion rate as its Mn^{2+}concentration is lower than that of other groups in the experiment.

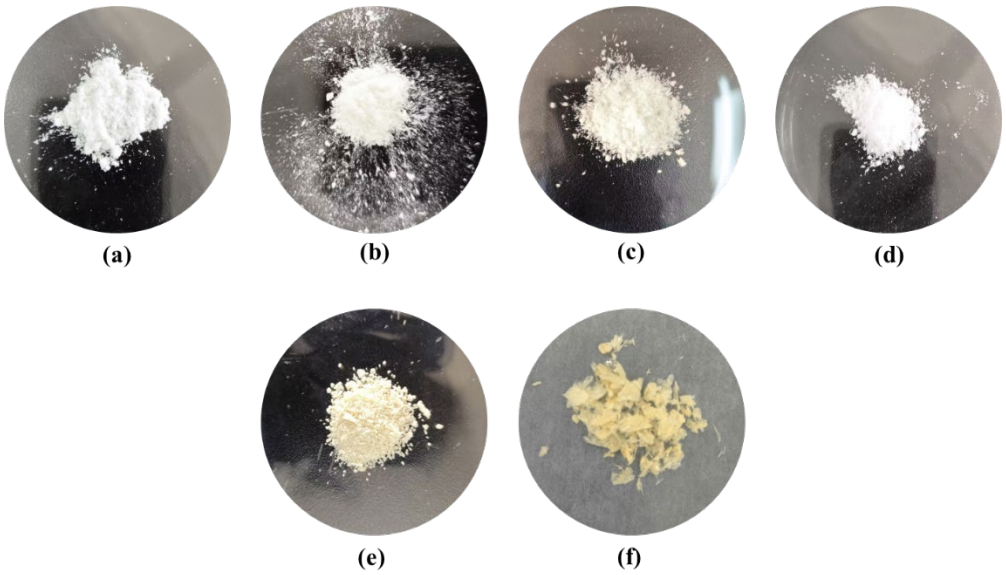

Figure. S7. Products of (a) MnO, (b) Mn_3O_4, (c) Mn_2O_3, and (d) MnO_2 synergized by $MnCl_2 \cdot 4H_2O$ at 180 ℃ for 1 hour, products of (e) 1wt% and (f) 10wt% of $MnCl_2 \cdot 4H_2O$ alone at 180 ℃ for 1 hour.

Note: Although increasing the loading of homogeneous $MnCl_2 \cdot 4H_2O$ from 1% to 10% could achieve complete PET degradation, the DMT selectivity dropped substantially (Fig. S5c), and the product color turned intensely yellow (Fig. S7e and S7f). In contrast, the synergistic system not only achieved efficient degradation but also yielded nearly white products (Fig. S7a-d), demonstrating its combined advantages in selectivity and product purity.

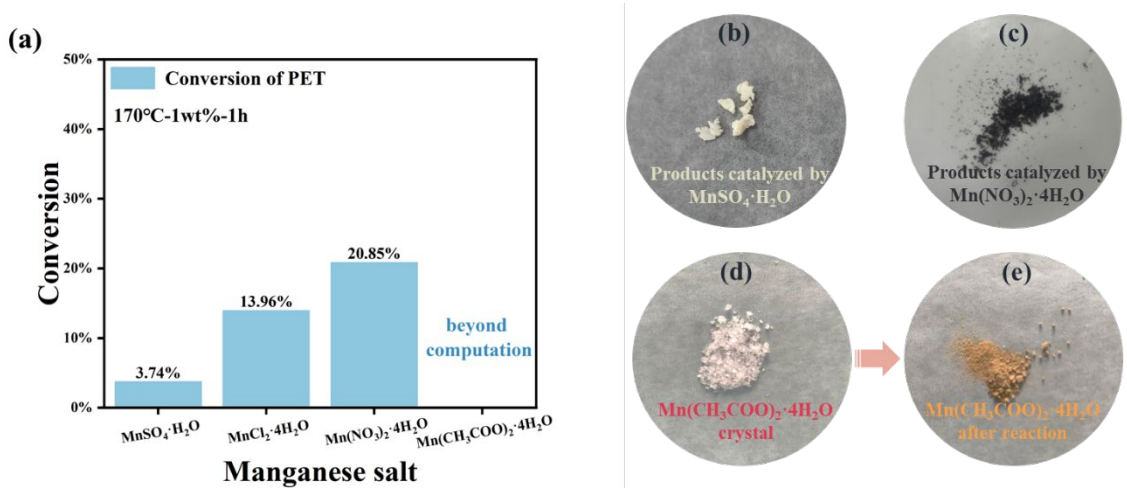

Figure. S8. (a) Degradation rate of PET catalyzed by different manganese salts; products of PET catalyzed by (b) $MnSO_4 \cdot H_2O$ and (c) $Mn(NO_3)_2 \cdot 4H_2O$; $Mn(CH_3COO)_2 \cdot 4H_2O$ (d) before and (e) after reaction.

Note: Fig. (a) shows the degradation efficiency using the homogeneous catalyst alone at 170 °C for 1 hour. For tetrahydrate manganese acetate, the formation of a brownish-yellow new species prevented the calculation of the conversion rate based on the mass difference of solids before and after the reaction. Figs. (b) and (c) present the products from PET depolymerization by hydrated manganese sulfate and tetrahydrate manganese nitrate, respectively. Figs. (d) and (e) provide a comparative view of the samples before and after the reaction with tetrahydrate manganese acetate.

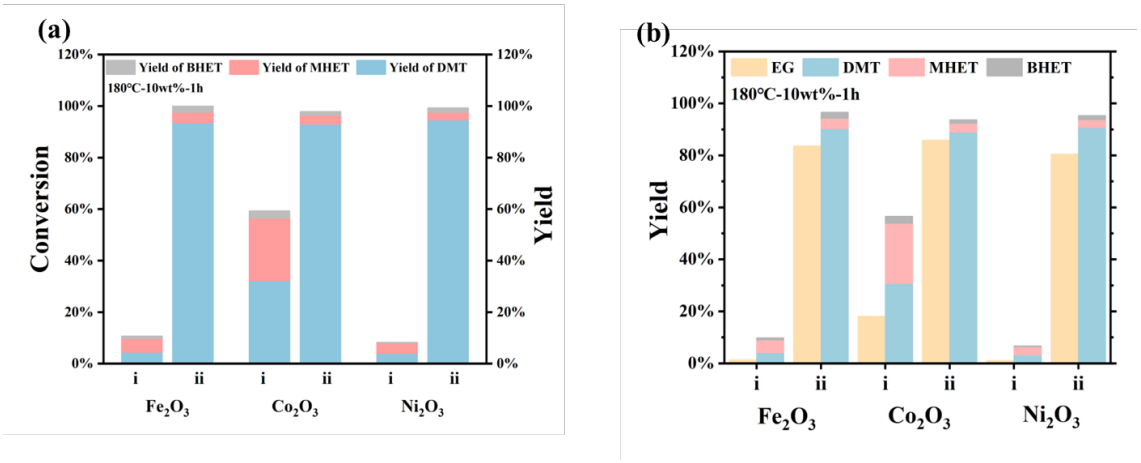

Figure. S9. Degradation rate of PET and yield of products catalyzed by different metal oxide and its corresponding synergistic systems, calculated by (a) normalization method and (b) internal standard method, respectively.

Note: The experimental conditions are 180 ℃-1 h, with 1 g PET , 0.1 g catalyst and 40 mL MeOH, like the typical experiment. In the synergistic experiment corresponding to each oxide, the catalyst was still added in a homogeneous and heterogeneous ratio of 1:9, using $FeCl_3 \cdot 6H_2O$, $CoCl_2 \cdot 6H_2O$, and $NiCl_2 \cdot 6H_2O$ as the homogeneous component, respectively. Similarly, ‘i’ denotes the single oxide system and ‘ii’ denotes the synergistic system.

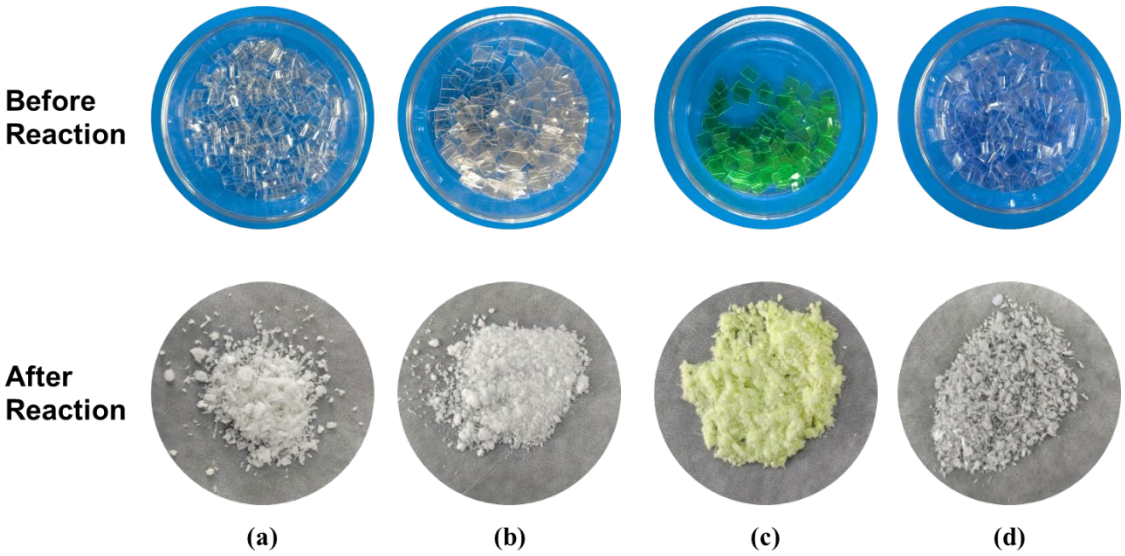

Figure. S10. Comparison of commercial plastics before and after reactions. (a) NoFu Spring, (b) Coca-Cola, (c) Sprite, (d) Mizone

Note: Commercial PET is cut into fragments and washed before being used for reaction

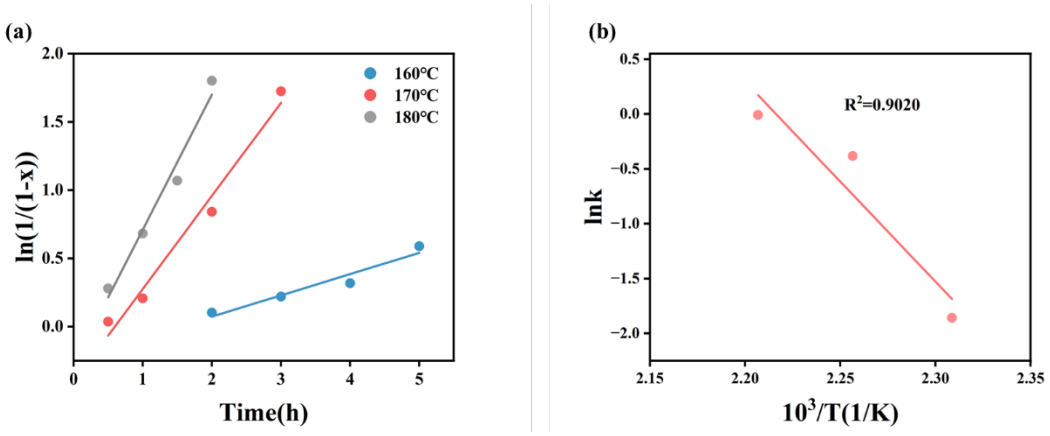

Figure. S11. (a) First-order kinetics at different temperatures; (b) Arrhenius diagram of the rate constant for PET methanolysis.

Note: To provide fundamental data for industrial process simulation (Aspen), kinetic studies were conducted on the $Mn_2O_3/MnCl_2$ synergistic system. The reaction followed a first-order kinetic model. Fitting the data with the Arrhenius equation yielded an apparent activation energy (Ea) of 151.61 kJ/mol for this synergistic degradation process. The catalyst proportion was reduced to 1% of the PET mass at 180 °C due to the PET conversion rate can reach 100% in a short period of time when 10wt% total catalyst was fed.

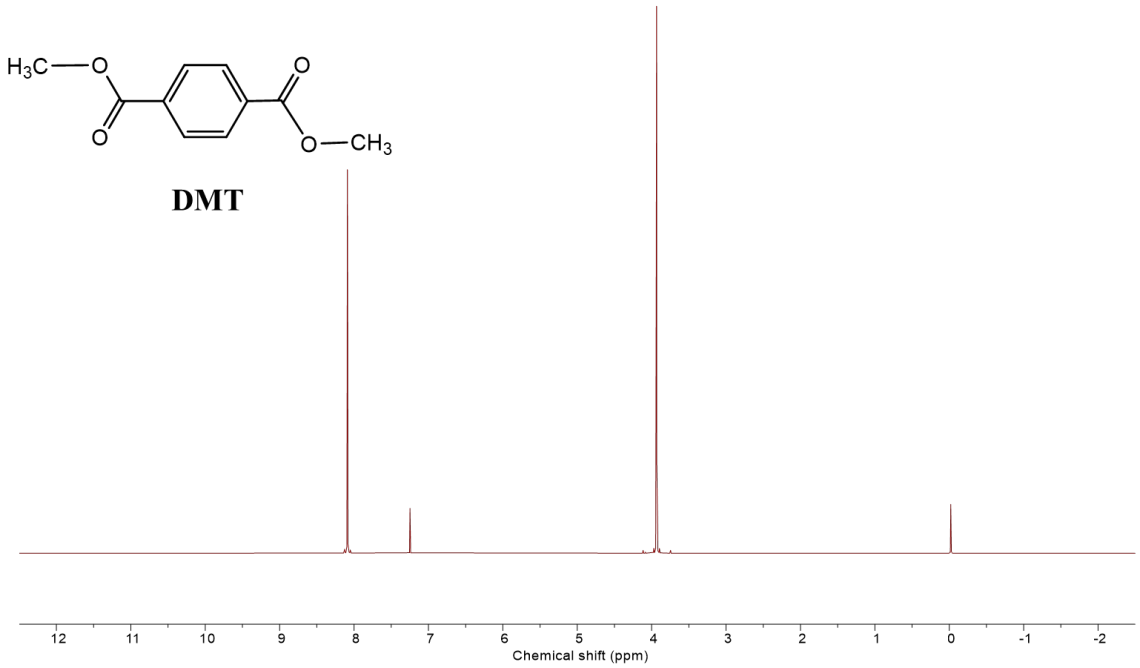

Figure. S12. ^{1}H NMR spectrum of pure DMT.

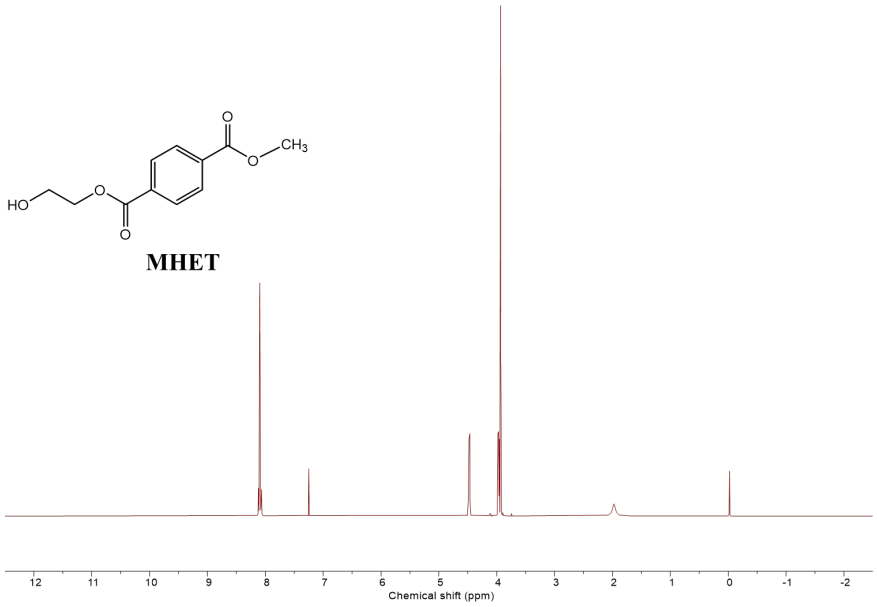

Figure. S13. ^{1}H NMR spectrum of pure MHET.

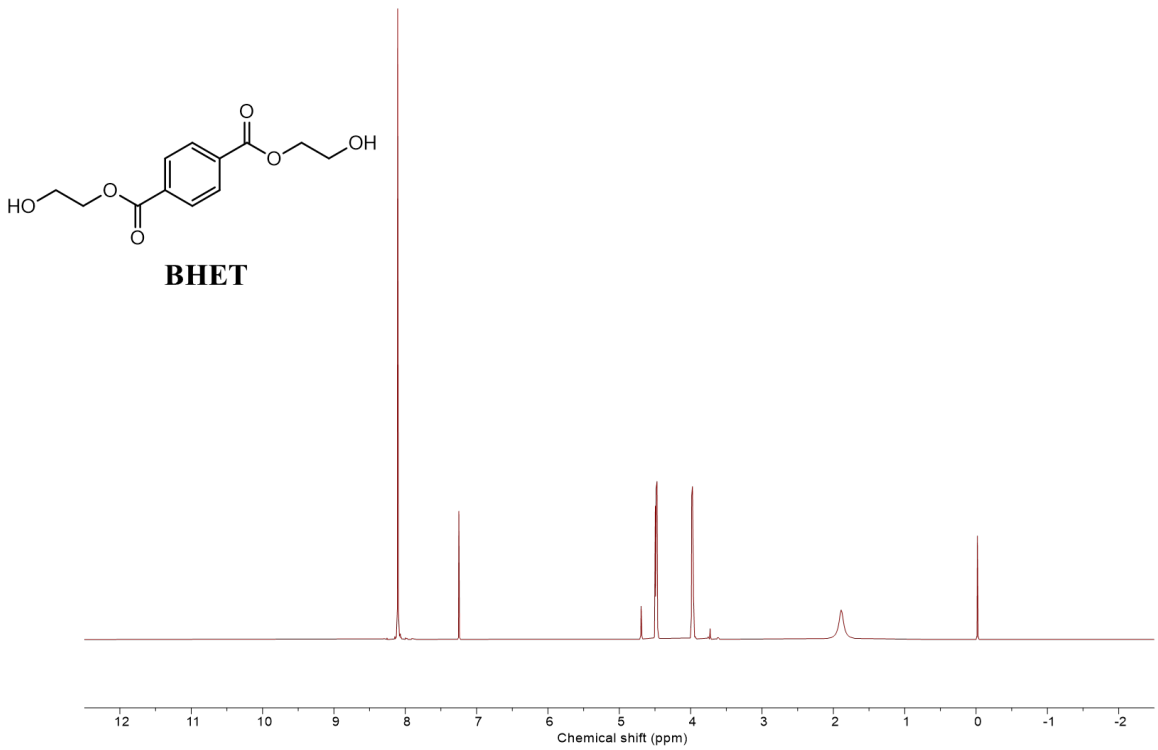

Figure. S14. ^{1}H NMR spectrum of pure BHET.

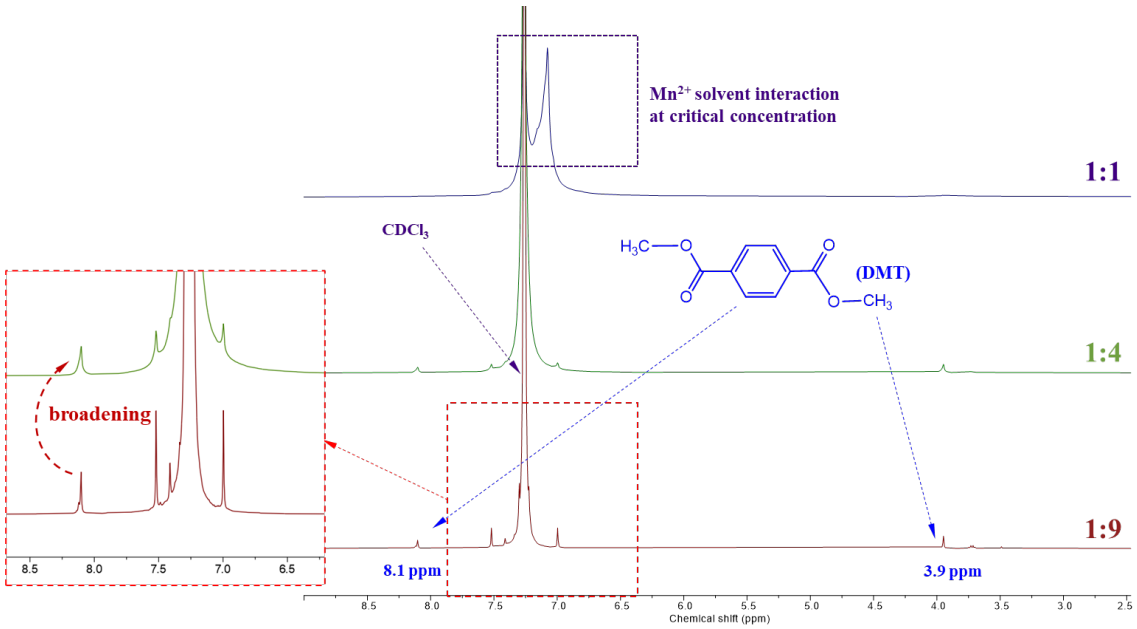

Figure. S15. ^{1}H NMR spectrum of products catalyzed by different mass ratios of $MnCl_2 \cdot 4H_2O$ and Mn_2O_3 (170 ℃-10wt% catalyst).

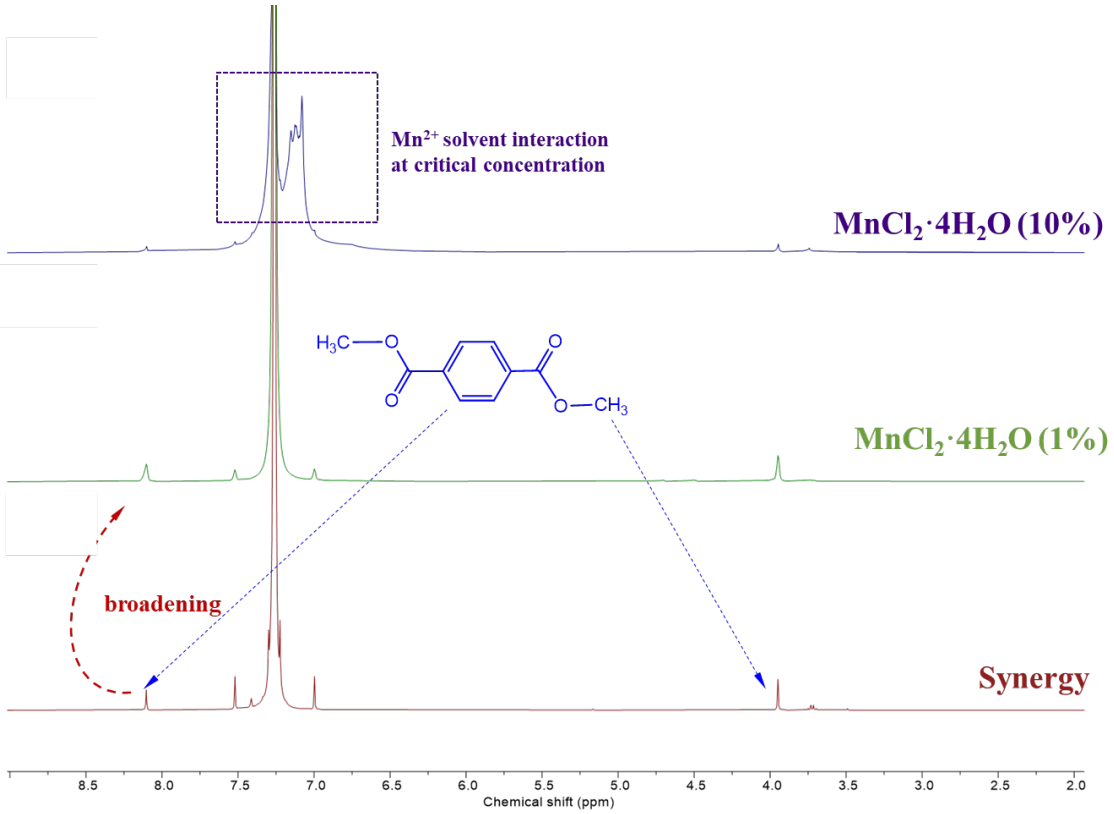

Figure. S16. ^{1}H NMR spectrum of products catalyzed by synergistic system and different dosage of $MnCl_2 \cdot 4H_2O$ at 180 ℃.

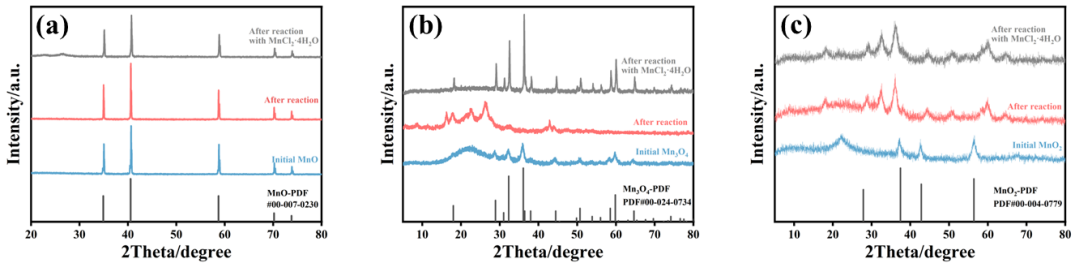

Figure. S17. XRD patterns of (a) MnO (b) Mn_3O_4 (c) MnO_2 before and after reaction.

Note: The crystal structures of the catalysts were characterized by X-ray diffraction using a Mini Flex 600 diffractometer. The measurements were performed with Cu Kα1 radiation (λ = 1.54 Å) at an operating voltage of 40 kV. Data were collected in the 2θ range of 5° to 80° with a step size of 0.02° and a scan rate of 5°/min. The obtained XRD patterns were analyzed using Jade software, and phase identification was achieved by comparing the diffraction patterns with standard reference cards (PDF database).

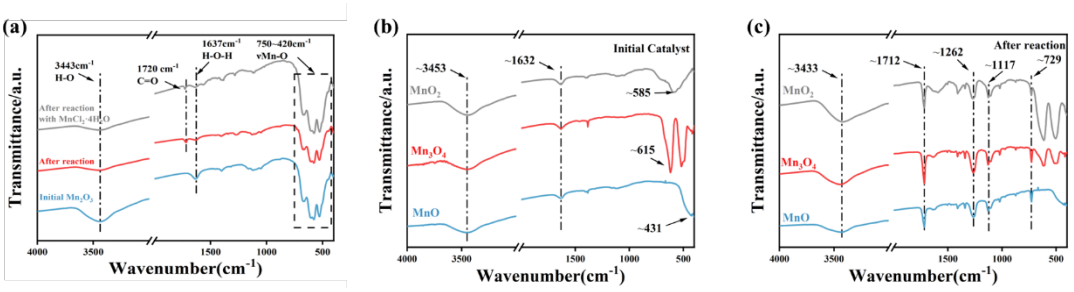

Figure. S18. (a) Infrared spectra of Mn_2O_3 before and after reaction; infrared spectra of MnO_x before (b) and after (c) synergistic reaction.

*Note:*For Fourier-Transform Infrared (FT-IR) analysis, samples were prepared using the standard KBr pellet method. A small amount of the sample was mixed and thoroughly ground with approximately 120 mg of potassium bromide (KBr). The homogeneous mixture was then pressed into a thin, transparent pellet under a pressure of 10 bar for about 15 seconds. The resulting pellet was subsequently analyzed in transmission mode to collect the infrared absorption spectrum.

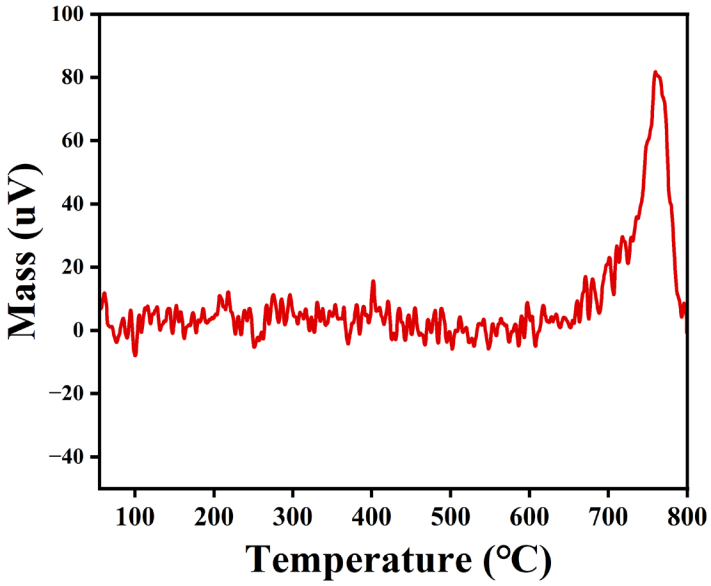

Figure. S19. CO_2-TPD spectra of Mn_2O_3.

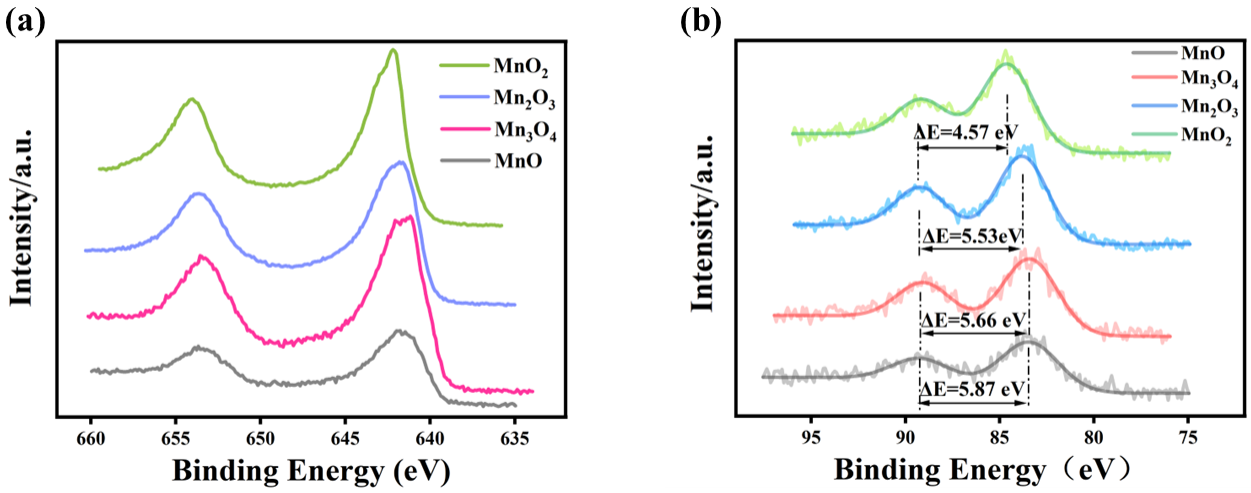

Figure. S20. Original XPS curves of MnO_x: (a) Mn 2p, (b) Mn 3s.

Note: The characterization parameters of XPS were as follows: the X-ray excitation source was monochromatic Al-Kα radiation (1486.6 eV), operating at 12 kV with a pass energy of 150.0 eV and a step size of 1 eV. The acquired data were processed using Avantage V6.9 software. The binding energy scale was calibrated by referencing the standard C 1s peak at 284.8 eV. The spectra were fitted using a Gaussian-Lorentzian (G-L) Model, and this same fitting procedure was applied to all subsequent data analysis unless otherwise specified.

To analyze the manganese oxidation states, we examined both the Mn 2p and Mn 3s core-level spectra. For the Mn 2p region, the spectrum typically presents as a broad envelope with multiple features. This complexity arises from the strong exchange interaction between the 3d electrons and the 2p core hole, leading to multiplet splitting. Additionally, the covalent character of the Mn–O bond can result in charge transfer satellite peaks due to partial screening of the core hole by ligand (O 2p) electrons. Consequently, the subtle differences in the Mn 2p line shapes among various manganese oxides make unambiguous determination of the oxidation state challenging from this region alone.In contrast, the Mn 3s spectrum consistently shows a well-resolved doublet, which is less susceptible to chemical environment effects. The splitting energy (ΔE) between these two peaks originates from the exchange coupling between the 3s core hole and the unpaired electrons

in the 3d orbital. As the manganese oxidation state increases, the number of unpaired 3d electrons decreases, weakening this exchange interaction and causing a systematic reduction in ΔE. Therefore, the Mn 3s doublet provides a more reliable metric for determining the average manganese oxidation state.

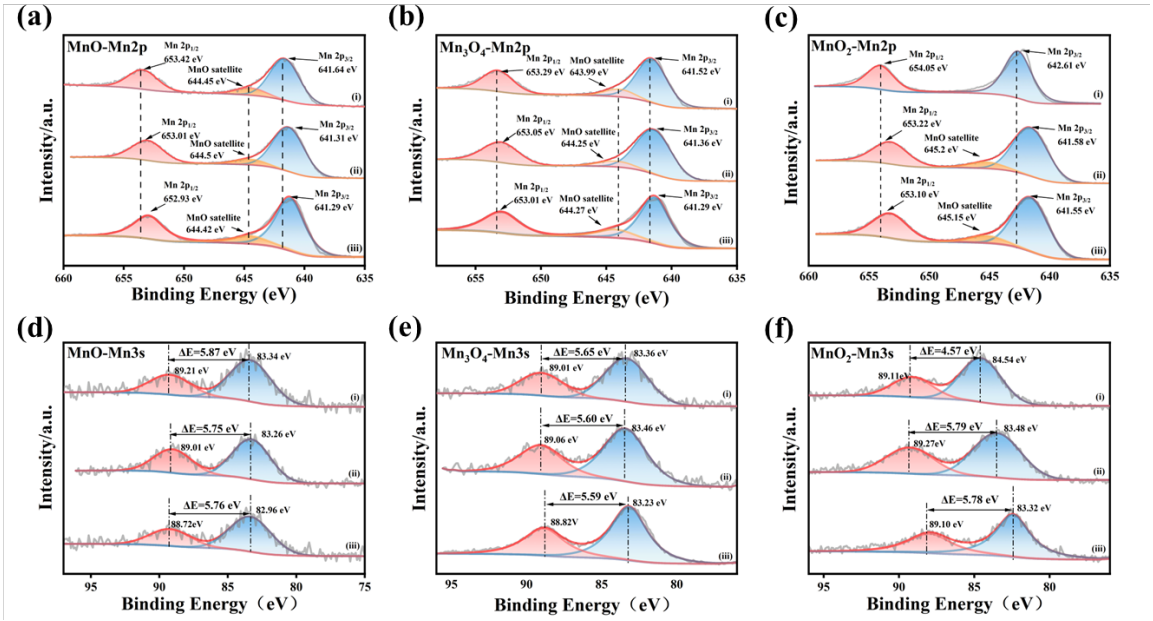

Figure. S21. XPS curves of Mn 2p: (a) MnO (b) Mn_3O_4 (c) MnO_2, and Mn 3s: (d) MnO (e) Mn_3O_4 (f) MnO_2. ((i) before reaction, (ii) after heterogeneous reaction, (iii) after synergistic reaction).

Note: For MnO and Mn_3O_4, the slight change in their Mn 3s ΔE value indicates that their leaching in methanol primarily occurs at the material surface. This surface process suggests they cannot maintain their activity over prolonged high-temperature reactions. In contrast, for MnO_2, the manganese valence state directly changed from +4 to a mixed +2/+3 state. This observation further underscores the superior stability of the +3 oxidation state (as in Mn_2O_3) in the methanolysis environment.

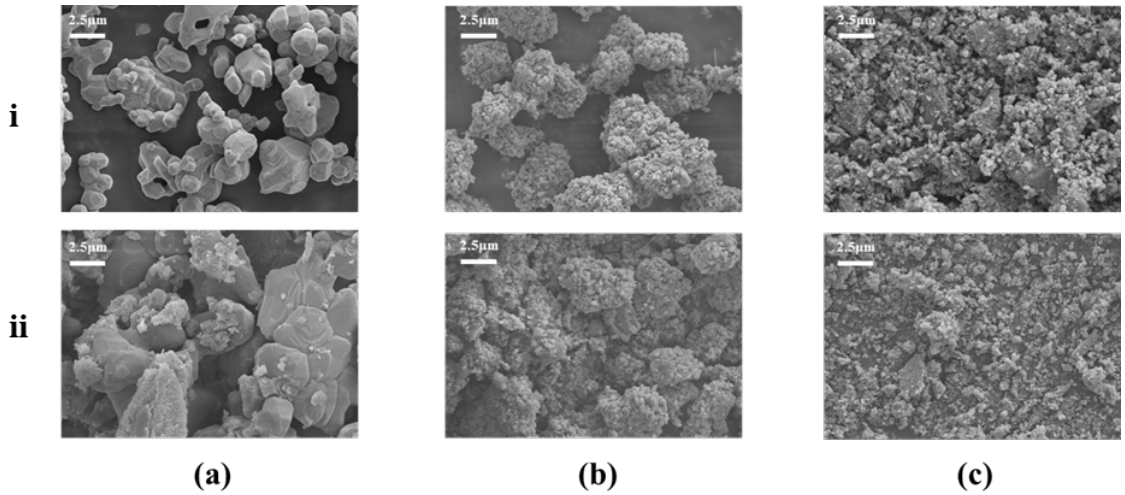

Figure. S22. SEM image of (a) MnO, (b) Mn_3O_4, (c) MnO_2 (i) before and (ii) after synergistic reaction.

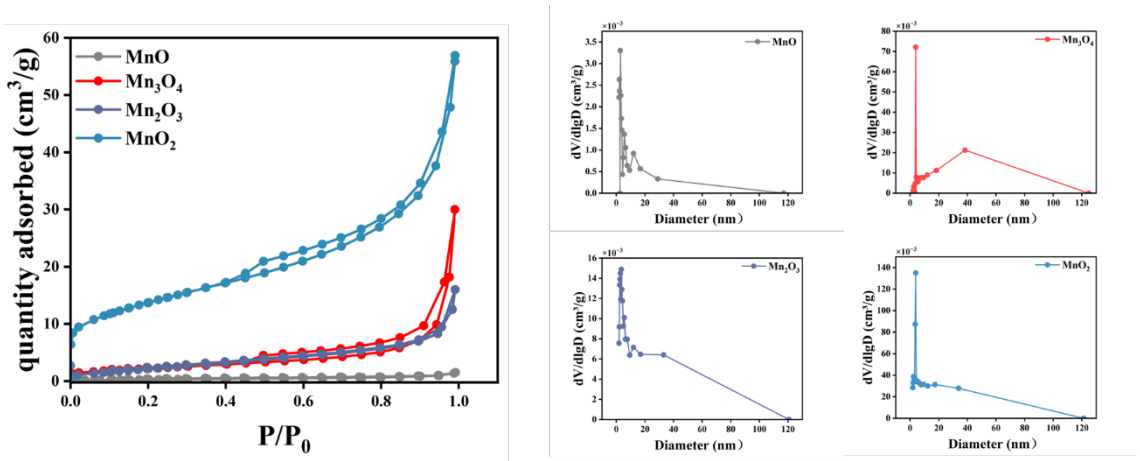

Figure. S23. N_2 adsorption-desorption isotherms of MnO_x.

Note: The textural properties of various MnO_x catalysts were characterized by N_2 adsorption-desorption measurements. The isotherm of Mn_2O_3 can be classified as type IV with a distinct H3 hysteresis loop, confirming its mesoporous structure. The corresponding pore size distribution, calculated using the Barrett-Joyner-Halenda (BJH) method, showed a sharp peak centered around 12 nm, indicating uniform mesopores. In comparison, MnO_2 and Mn_3O_4 also displayed type IV isotherms but with broader pore size distributions. MnO exhibited a characteristic type II isotherm with very low uptake, suggesting a nearly non-porous structure. The specific surface areas followed the order: MnO_2 > Mn_3O_4 > Mn_2O_3 > MnO. Therefore, Mn_2O_3 achieves an optimal trade-off between specific surface area and structural stability.

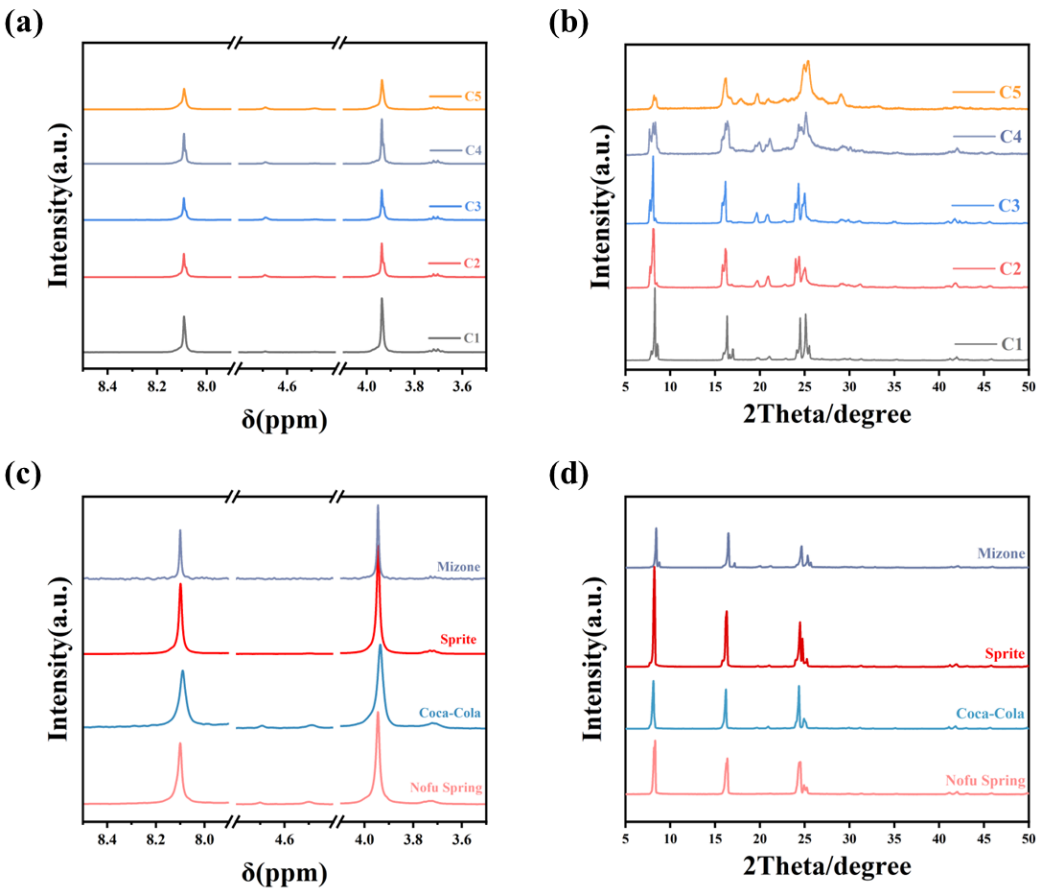

Figure. S24. (a) ^{1}H NMR spectra and (b) XRD patterns of products in each recycling cycles, (c) ^{1}H NMR spectra and (d) XRD patterns of commercial plastic products.

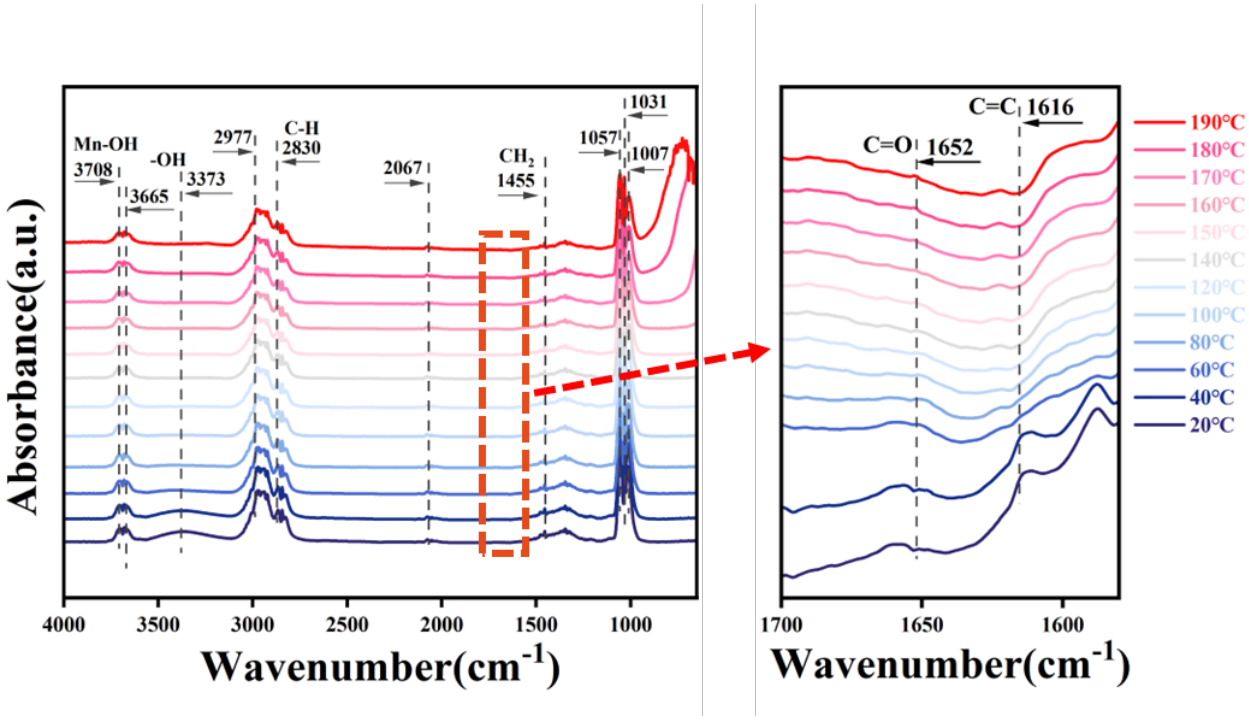

Figure. S25. *In-situ* DRIFTS of MnO alone .

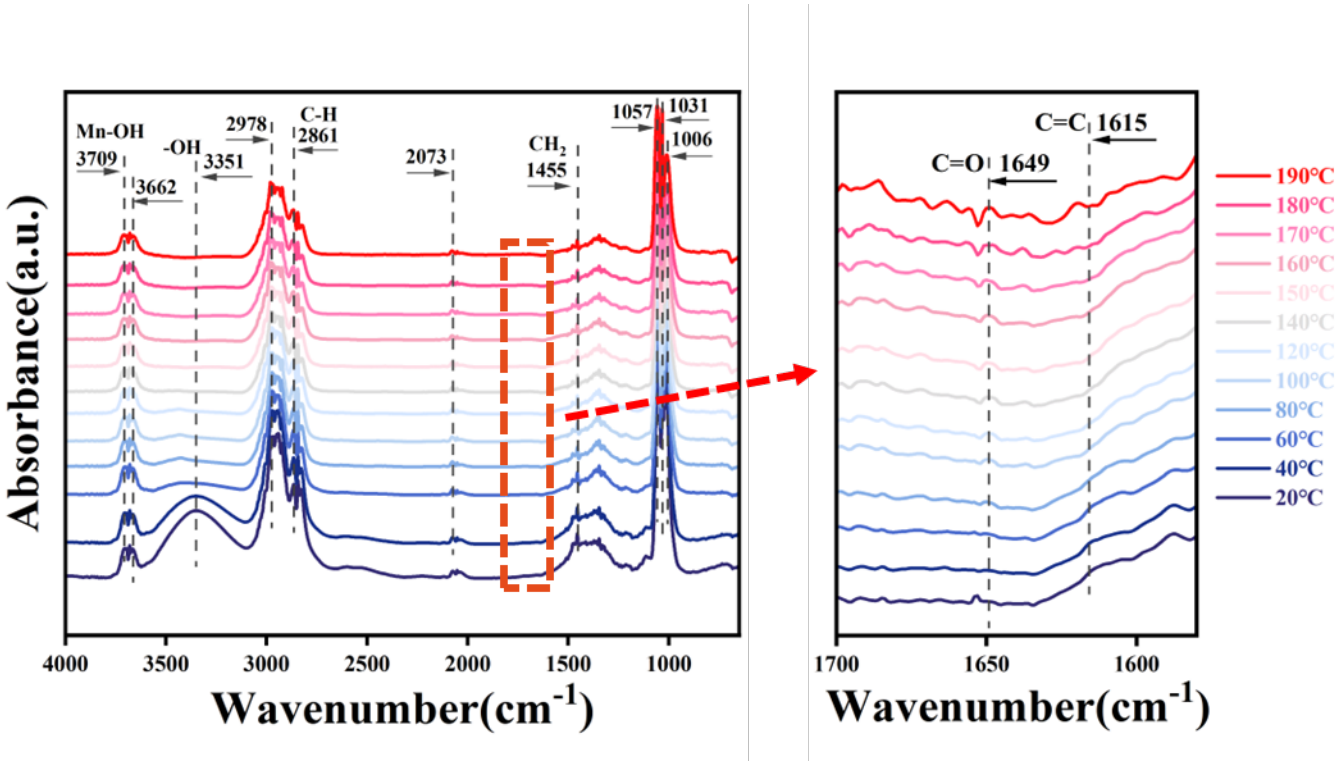

Figure. S26. *In-situ* DRIFTS of Mn_3O_4 alone.

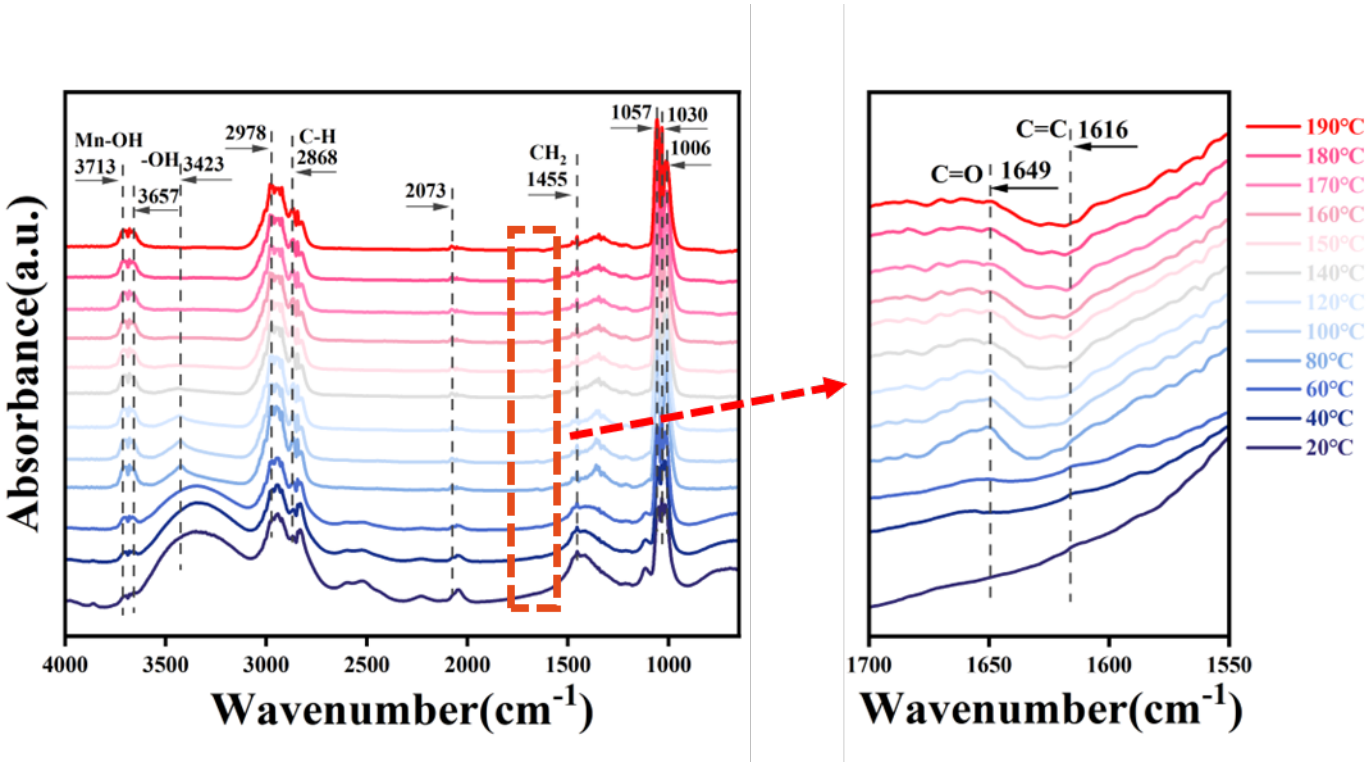

Figure. S27. *In-situ* DRIFTS of MnO_2 alone .

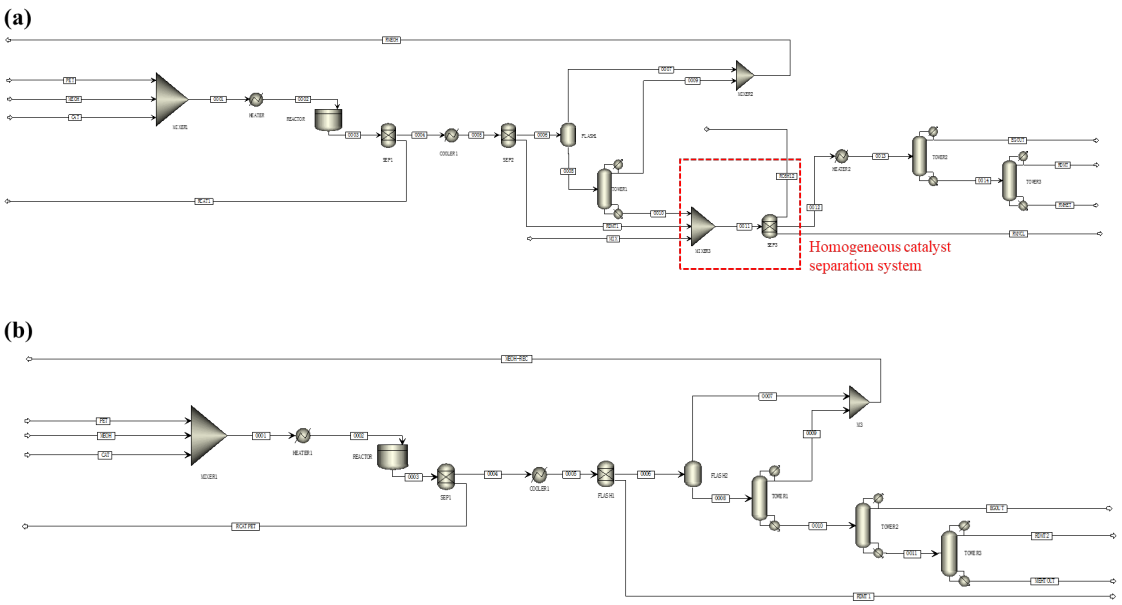

Figure. S28. Process simulation of PET methanolysis through (a) synergistic system and (b) heterogeneous system by Aspen Plus .

Note: The Aspen Plus simulation utilized a set of property databases including APV140 ASPENPCD, APV140 AQUEOUS, APV140 SOLIDS, APV140 INORGANIC, APESV140 AP-EOS, NISTV140 NIST-TRC, APV140 POLYMER, and APV140 PURE40. The NRTL model was employed as the primary property method for handling the mixed organic system. For the homogeneous manganese salt section, the ELECNRTL method was applied to establish the necessary binary interaction parameters. Utility analysis was performed using the built-in utility module within Aspen Plus V14.

Process :As illustrated in Fig. S28a, the process flow for the synergistic system can be summarized as follows: First, PET particles, catalysts, and methanol are thoroughly mixed in Mixer 1 (MIXER-1). The mixture is preheated (HEATER-1) and then fed into a stirred batch reactor (REACTOR) for methanolysis. The post-reaction stream undergoes a preliminary separation at elevated temperature to recover the heterogeneous Mn_2O_3 catalyst. It is then cooled in Cooler 1 (COOLER-1) to crystallize and recover a portion of the DMT product (which carries some $MnCl_2$). The remaining liquid stream enters a flash drum (FLASH-1) to separate the majority of the methanol, followed by Distillation Column

1 (TOWER-1) to recover the remaining methanol overhead. The bottom product from TOWER-1, a mixture of DMT, byproducts, and a small amount of methanol, is combined with the crystallized DMT and fed into the homogeneous catalyst separation system to recover $MnCl_2$ (the outlet flow rate is derived from a separate Aspen process). The separated organic phase is then preheated and sent to Distillation Column 2 (TOWER-2), where ethylene glycol (EG) is recovered as the overhead product. The bottom stream from TOWER-2 enters Distillation Column 3 (TOWER-3) for final separation, yielding high-purity (99.99%) dimethyl terephthalate (DMT) and industrial-grade (91.96%) mono(2-hydroxyethyl) terephthalate (MHET) as products. For the heterogeneous-only system, the process omits the homogeneous catalyst separation unit, while the rest of the flow sheets remain consistent with the description above, the mass balance table of each stream of the two processes has been listed in Table S18-22.

Within the homogeneous catalyst separation system, a mixed solution of water and cyclohexane (mass ratio of 2:3) at a total flow rate of 10,000 kg/h was introduced for washing and phase separation. The final aqueous phase contained the $MnCl_2$ solution for recovery, while the organic phase, comprising cyclohexane mixed with the main and by-products, was directed to the subsequent separation processes.

Part 2 Supplementary Tables

Table. S1. Conversion of PET and yield of products (170 ℃-10wt%-1h).

Catalysts	Category	Conversion of PET	Yield (normalization method)			Yield (internal standard method)			Yield
			DMT	MHET	BHET	DMT	MHET	BHET	EG
MnO	**i**	11.43%	8.09%	2.14%	1.20%	6.37%	1.69%	0.94%	2.93%
MnO	**ii**	71.67%	64.01%	5.13%	2.53%	60.03%	4.81%	2.37%	51.36%
Mn_3O_4	**i**	5.92%	5.92%	0.31%	0.19%	5.29%	0.31%	0.18%	4.09%
Mn_3O_4	**ii**	51.02%	46.30%	3.09%	1.63%	41.30%	2.76%	1.45%	35.08%
Mn_2O_3	**i**	1.50%	1.13%	0.22%	0.15%	1.10%	0.21%	0.15%	1.13%
Mn_2O_3	**ii**	18.68%	11.15%	6.61%	0.91%	10.33%	6.13%	0.84%	2.84%
MnO_2	**i**	13.78%	10.23%	2.46%	1.09%	8.52%	2.05%	0.91%	4.66%
MnO_2	**ii**	73.37%	66.84%	1.96%	4.57%	59.33%	1.74%	4.05%	48.71%

Note: Supplementary Tables S1-7 present the raw data for the conversion of PET methanolysis and the corresponding product yields, calculated based on the normalization method and internal standard method. In Table. S1 and Table. S2, 'i' represents the individual oxide system, while 'ii' represents the synergistic system. The total catalyst mass is 10% of the PET mass.

Table. S2. Conversion of PET and yield of products (180 ℃-10wt%-1h).

Catalysts	Category	Conversion of PET	Yield (normalization method)			Yield (internal standard method)			Yield
			DMT	MHET	BHET	DMT	MHET	BHET	EG
MnO	**i**	76.01%	54.70%	19.39%	1.92%	49.34%	17.49%	1.73%	28.33%
MnO	**ii**	100.00%	95.00%	1.90%	3.10%	93.40%	1.87%	3.05%	86.39%
Mn_3O_4	**i**	9.49%	4.63%	4.03%	0.82%	4.11%	3.58%	0.73%	1.67%
Mn_3O_4	**ii**	100.00%	96.47%	1.29%	2.24%	93.38%	1.25%	2.17%	88.97%
Mn_2O_3	**i**	8.79%	4.20%	4.59%	0.00%	3.85%	4.21%	0.00%	2.28%
Mn_2O_3	**ii**	100.00%	95.35%	1.75%	2.90%	93.97%	1.73%	2.86%	85.72%
MnO_2	**i**	89.55%	80.12%	6.34%	3.08%	76.86%	6.08%	2.96%	66.87%
MnO_2	**ii**	100.00%	95.23%	1.83%	2.94%	94.06%	1.81%	2.91%	89.17%

Note: The total catalyst mass is 10% of the PET mass.

Table. S3. Conversion of PET and yield of products at different times at 170 ℃.

Time (h)	Conversion of PET	Yield (normalization method)			Yield (internal standard method)			Yield
		DMT	MHET	BHET	DMT	MHET	BHET	EG
0.5	3.60%	2.82%	0.58%	0.20%	2.17%	0.45%	0.15%	1.72%
1	18.68%	11.15%	6.61%	0.91%	10.33%	6.13%	0.84%	2.84%
2	56.90%	46.13%	7.48%	3.30%	42.68%	6.92%	3.05%	31.47%
3	82.16%	78.64%	2.03%	1.48%	74.94%	1.94%	1.41%	69.82%
4	99.98%	96.53%	1.23%	2.22%	92.95%	1.18%	2.14%	89.17%
6	100.00%	96.60%	1.11%	2.29%	94.88%	1.09%	2.25%	90.03%

Note: The total catalyst mass is 10% of the PET mass.

Table. S4. Conversion of PET and yield of products at different mass ratios ($MnCl_2 \cdot 4H_2O$: Mn_2O_3) at 170 ℃.

Ratio	Conversion of PET	Yield (normalization method)			Yield (internal standard method)			Yield
		DMT	MHET	BHET	DMT	MHET	BHET	EG
1:36	3.51%	1.39%	1.31%	0.81%	1.06%	1.00%	0.62%	0
1:18	5.89%	2.19%	2.12%	1.58%	1.97%	1.92%	1.43%	0
1:9	18.68%	11.15%	6.61%	0.91%	10.33%	6.13%	0.84%	2.84%
1:4	40.11%	30.62%	7.27%	2.22%	26.76%	6.36%	1.94%	18.53%
1:1	34.84%	28.30%	4.08%	2.46%	26.15%	3.77%	2.28%	19.21%
4:1	31.81%	26.90%	3.42%	1.48%	23.58%	3.00%	1.30%	17.83%
1	30.62%	21.63%	4.59%	4.40%	18.44%	3.91%	3.75%	7.52%

Note: The total catalyst mass is 10% of the PET mass.

Table. S5. Conversion of PET and yield of products at different temperatures when $MnCl_2 \cdot 4H_2O$ used alone.

Temperature (℃)	Dosage	Conversion of PET	Yield (normalization method)			Yield (internal standard method)			Yield
			DMT	MHET	BHET	DMT	MHET	BHET	EG
170	1%	13.96%	8.17%	3.81%	1.98%	4.26%	1.99%	1.03%	1.22%
	10%	30.62%	21.63%	4.59%	4.40%	18.44%	3.91%	3.75%	7.52%
180	1%	58.02%	32.71%	21.24%	4.07%	28.85%	18.74%	3.59%	5.94%
	10%	100.00%	65.54%	24.59%	9.87%	60.71%	22.78%	9.14%	28.65%

Note: The reaction time is 1 hour.

Table. S6. Conversion of PET and product yields over repeated catalyst recycling.

Cycle method	Cycle times	Conversion of PET	Yield (normalization method)			Yield (internal standard method)			Yield
			DMT	MHET	BHET	DMT	MHET	BHET	EG
Semi-supplementation strategy	C1	73.37%	68.39%	2.35%	2.63%	66.36%	2.28%	2.55%	59.98%
	C2	70.42%	68.38%	1.36%	0.68%	65.27%	1.30%	0.65%	62.47%
	C3	67.36%	65.37%	1.86%	0.13%	63.97%	1.82%	0.13%	60.76%
	C4	73.25%	70.39%	2.12%	0.74%	67.57%	2.04%	0.71%	63.17%
	C5	69.85%	66.48%	3.14%	0.23%	62.17%	2.94%	0.22%	58.83%
Recycled Mn_2O_3 + fresh $MnCl_2{\cdot}4H_2O$	C1	97.26%	93.64%	2.35%	1.27%	90.83%	2.28%	1.23%	87.21%
	C2	98.12%	91.33%	3.98%	2.81%	88.15%	3.84%	2.71%	79.36%
	C3	96.85%	92.66%	2.33%	1.86%	87.24%	2.20%	1.75%	76.25%
Recycled Mn_2O_3 + recycled $MnCl_2{\cdot}4H_2O$	C1	74.46%	68.25%	3.88%	2.33%	68.44%	3.89%	2.34%	53.34%
	C2	68.51%	63.33%	4.15%	1.03%	58.62%	3.84%	0.95%	49.82%
	C3	61.32%	54.27%	4.76%	2.29%	52.36%	4.59%	2.21%	46.73%

Note: The reaction time is 1 hour and the total catalyst mass is 10% of the PET mass. The method of catalyst recycling by "semi-supplementation" is shown in note of Fig. S5.

Table. S7. Conversion of commercial PET and yield of products at 180 ℃ for 1 hour.

Category	Conversion of PET	Yield (Normalization Method)			Yield (internal standard method)			Yield
		DMT	MHET	BHET	DMT	MHET	BHET	EG
Nongfu Spring	100.00%	97.38%	2.06%	0.56%	96.32%	2.04%	0.55%	93.07%
Coca-Cola	98.09%	94.89%	2.79%	0.41%	92.21%	2.71%	0.39%	89.36%
Sprite	97.45%	94.96%	1.06%	1.43%	94.25%	1.05%	1.42%	91.45%
Mizone	99.59%	95.98%	3.08%	0.53%	93.13%	2.99%	0.52%	89.61%

Note: The total catalyst mass is 10% ($MnCl_2 \cdot 4H_2O$: Mn_2O_3=1:9) of the PET mass.

Table. S8. Conversion of PET and yield of products with different volumes of methanol at 180 ℃ for 1 hour.

MeOH (mL)	Conversion of PET	Yield (Normalization Method)			Yield (internal standard method)			Yield
		DMT	MHET	BHET	DMT	MHET	BHET	EG
10	91.64%	84.38%	6.53%	0.73%	81.72%	6.32%	0.71%	69.06%
20	97.61%	94.32%	2.34%	0.95%	91.61%	2.02%	0.92%	87.10%
40	100.00%	95.35%	1.75%	2.90%	93.97%	1.73%	2.86%	85.27%
80	88.63%	85.37%	2.80%	0.46%	83.76%	2.75%	0.45%	81.34%

Note: The method of different volumes loading is shown in note of Fig. S6.

Table. S9. Conversion of PET and yield of products with different catalyst loading at 180 ℃ for 1 hour.

Catalyst loading	Conversion of PET	Yield (Normalization Method)			Yield (internal standard method)			Yield
		DMT	MHET	BHET	DMT	MHET	BHET	EG
1%	49.42%	40.98%	7.13%	1.31%	39.14%	6.81%	1.25%	28.99%
2.5%	76.14%	66.93%	6.45%	2.76%	65.83%	6.34%	2.71%	56.08%
5%	94.28%	89.63%	3.55%	1.10%	89.11%	3.53%	1.09%	82.15%
10%	100.00%	95.35%	1.75%	2.90%	93.97%	1.73%	2.86%	85.27%

Table. S10. Conversion of PET and yield of products with heterogeneous ('i') and synergistic ('ii') system for oxidation with other transition metals.

Metal oxide	Category	Conversion of PET	Yield (normalization method)			Yield (internal standard method)			Yield
			DMT	MHET	BHET	DMT	MHET	BHET	EG
Fe_2O_3	i	10.71%	4.39%	5.31%	1.01%	4.04%	4.89%	0.93%	1.33%
	ii	100.00%	93.38%	4.15%	2.47%	90.24%	4.01%	2.39%	83.64%
Co_2O_3	i	59.36%	32.14%	24.31%	2.91%	30.65%	23.18%	2.78%	18.11%
	ii	97.89%	92.88%	3.51%	1.50%	88.92%	3.36%	1.44%	85.83%
Ni_2O_3	i	8.31%	3.89%	3.97%	0.45%	3.14%	3.20%	0.36%	1.06%
	ii	99.39%	94.47%	3.10%	1.76%	90.66%	2.97%	1.69%	80.46%

Table. S11. Residual metal content in the solution catalyzed by metal oxides

Metal oxide	Residual amount of metal in solution (mg/L)
Fe_2O_3	Not detected
Co_2O_3	5.42
Ni_2O_3	1.61

Note: The measuring elements were Fe, Co, and Ni, respectively.

Table. S12. Residual manganese content in the product before and after washing

Mass ratio of $MnCl_2·4H_2O$: Mn_2O_3	**Washing time**	**Residual manganese (mg/kg)**
1:9	0	2790
	3	70.1
	5	29.5
	10	27.2
1:4	0	20900
	3	369
	5	270
	10	189

Note: The product listed in the table is obtained at 180 ℃ for 1 hour. As can be seen from the table, when the number of water washing cycles increased to 10, the removal rate of residual manganese reached approximately 99% for all mass ratios of $MnCl_2·4H_2O$ to Mn_2O_3. This confirms that excessive homogeneous $MnCl_2·4H_2O$ will inevitably impair the final product purity.

Table. S13. Ratio of $MnCl_2 \cdot 4H_2O$ in different catalytic systems (comparation of mass and molar ratio), with 10wt% total catalyst of PET.

Catalyst system	Mass ratio ($MnCl_2 \cdot 4H_2O$: MnO_x)	Molar ratio
$MnO + MnCl_2 \cdot 4H_2O$	1 : 9	1 : 17.2
$Mn_3O_4 + MnCl_2 \cdot 4H_2O$	1 : 9	1 : 14.8
$Mn_2O_3 + MnCl_2 \cdot 4H_2O$	**1 : 9**	**1 : 11.3**
$MnO_2 + MnCl_2 \cdot 4H_2O$	1 : 9	1 : 20.5

Table. S14. MnO XPS spectral fitting.

	Peak Name		Peak position	Height (CPS)	Area CPS.eV	FWHM (eV)
i	Mn 2p	2p 3/2	641.56	10744.17	35138.70	3.14
		2p 1/2	653.68	5064.36	16886.36	3.20
		satellite	645.98	984.78	2729.49	2.66
	Mn 3s		83.31	1183.44	3784.80	3.07
			89.30	661.72	2854.52	4.14
ii	Mn 2p	2p 3/2	641.24	23003.69	79697.18	3.32
		2p1/2	653.08	10520.20	34420.16	3.14
		satellite	646.06	1553.49	4241.04	2.62
	Mn 3s		83.33	1920.56	6048.39	3.02
			89.17	1224.68	3879.33	3.04
iii	Mn 2p	2p 3/2	641.19	30776.28	96865.06	2.91
		2p1/2	652.93	13687.63	47545.68	2.99
		satellite	644.42	4661.08	20263.23	3.50
	Mn 3s		82.96	2618.06	8882.43	3.05
			88.72	1288.89	4731.10	3.50

Note: Table S14-17 provide the raw XPS fitting data for manganese, with the corresponding fitting methodology detailed in Fig. S19. Here, ‘i’ represents the original catalyst, ‘ii’ represents the catalyst after heterogeneous system reaction, and ‘iii’ represents the catalyst after synergistic reaction, the same of Table S15-17.

Table. S15. Mn_3O_4 XPS spectral fitting.

	Peak Name		Peak position	Height (CPS)	Area CPS.eV	FWHM (eV)
i	Mn 2p	2p 3/2	641.51	25915.99	86299.17	3.20
		2p 1/2	653.50	12103.27	40861.03	3.24
		satellite	646.15	2162.37	6241.27	2.77
	Mn 3s		83.36	2261.67	6949.20	2.95
			88.98	1474.79	3657.38	2.38
ii	Mn 2p	2p 3/2	641.39	26552.31	96384.61	3.48
		2p 1/2	653.07	12199.04	42958.67	3.38
		satellite	646.02	2337.60	8695.63	3.57
	Mn 3s		83.46	2119.25	9654.80	3.14
			89.06	911.35	3398.49	3.48
iii	Mn 2p	2p 3/2	641.26	156214.63	472814.34	2.90
		2p 1/2	653.01	74595.13	251497.31	3.03
		satellite	644.05	35471.69	144178.15	3.50
	Mn 3s		83.23	2058.06	7799.77	3.50
			88.82	1117.09	4232.29	3.50

Table. S16. Mn_2O_3 XPS spectral fitting.

	Peak Name		Peak position	Height (CPS)	Area CPS.eV	FWHM (eV)
i	Mn 2p	2p 3/2	653.55	28039.62	104082.11	3.36
		2p 1/2	641.69	55488.23	201282.28	2.32
	Mn 3s		83.46	4105.35	14800.84	2.16
			88.99	1915.05	8131.77	2.38
ii	Mn 2p	2p 3/2	641.21	3609.67	14524.40	2.36
		2p 1/2	653.24	1758.82	6863.39	3.50
	Mn 3s		83.70	321.60	1218.81	3.50
			89.21	180.87	685.39	3.50
iii	Mn 2p	2p 3/2	641.11	23511.24	88897.53	2.23
		2p 1/2	653.07	11470.71	43668.03	3.45
	Mn 3s		83.61	1920.16	6873.74	2.73
			89.14	888.35	3712.89	3.50

Table. S17. MnO_2 XPS spectral fitting.

	Peak Name		Peak position	Height (CPS)	Area CPS.eV	FWHM (eV)
i	Mn 2p	2p 3/2	642.61	88581.21	211518.40	2.67
		2p 1/2	654.05	68621.66	105759.20	2.67
	Mn 3s		84.54	9740.60	12500.74	3.17
			89.11	8130.03	5736.50	3.17
ii	Mn 2p	2p 3/2	641.58	72430.73	176518.40	3.39
		2p 1/2	653.22	58003.95	88259.20	3.38
		satellite	645.20	37502.73	26333.60	3.38
	Mn 3s		83.48	8975.51	13652.78	3.72
			89.27	7855.78	8055.56	3.71
iii	Mn 2p	2p 3/2	641.55	169440.93	537000.53	2.98
		2p 1/2	653.10	80686.16	296747.26	3.09
		satellite	645.15	27798.69	120526.42	4.12
	Mn 3s		83.32	12960.36	42967.14	2.98
			89.10	6976.52	29155.83	3.50

Table. S18. Mass balance of PET methanolysis in synergistic system.

Stream	CAT	MEOH	PET	0001	0002	0003	0004	0005
Temperature (℃)	25.0	25.0	25.0	25.1	180.0	180.0	180.0	30.0
Pressure (bar)	1.0	1.0	1.0	1.0	30.0	30.0	30.0	1.0
Mass flow (kg/hr)	2000.00	300000.00	20000.00	322000.00	322000.00	322048.69	320248.69	320248.69
PET	0.00	0.00	20000.00	20000.00	20000.00	0.00	0.00	0.00
CH3OH	0.00	300000.00	0.00	300000.00	300000.00	293433.62	293433.62	293433.62
MN2O3	1800.00	0.00	0.00	1800.00	1800.00	1800.00	0.00	0.00
EG	0.00	0.00	0.00	0.00	0.00	6244.21	6244.21	6244.21
BHET	0.00	0.00	0.00	0.00	0.00	29.50	29.50	29.50
MHET	0.00	0.00	0.00	0.00	0.00	783.21	783.21	783.21
DMT	0.00	0.00	0.00	0.00	0.00	19558.15	19558.15	19558.15
MNCL2	200.00	0.00	0.00	0.00	0.00	0.00	0.00	0.00
WATER	0.00	0.00	0.00	0.00	0.00	0.00	0.00	0.00
C6H12	0.00	0.00	0.00	0.00	0.00	0.00	0.00	0.00
Mn^{2+}	0.00	0.00	0.00	87.31	87.31	87.31	87.31	87.31
Cl^{-}	0.00	0.00	0.00	112.69	112.69	112.69	112.69	112.69

Table. S19. Mass balance of PET methanolysis in synergistic system (continued).

Stream	0006	0007	0008	0009	0010	0010	0011	0012	0013	0014
Temperature (℃)	30.0	70.0	70.0	58.9	208.7	208.7	86.2	86.2	200.0	302.3
Pressure (bar)	1.0	0.8	0.8	0.8	1.2	1.2	1.0	1.0	1.0	1.5
Mass flow (kg/hr)	305380.08	291392.68	13987.40	2922.10	11065.30	11065.30	35933.91	25734.82	25734.82	20300.77
PET	0.00	0.00	0.00	0.00	0.00	0.00	0.00	0.00	0.00	0.00
CH3OH	293433.62	290511.11	2922.51	2916.66	5.85	5.85	5.85	0.00	0.00	0.00
MN2O3	0.00	0.00	0.00	0.00	0.00	0.00	0.00	0.00	0.00	0.00
EG	6244.21	812.89	5431.32	5.43	5425.89	5425.89	5425.89	5424.64	5424.64	0.54
BHET	29.50	0.00	29.50	0.00	29.50	29.50	29.50	29.50	29.50	29.50
MHET	783.21	0.04	783.17	0.00	783.17	783.17	783.17	783.17	783.17	783.17
DMT	4889.54	68.64	4820.90	0.00	4820.90	4820.90	19489.51	19489.51	19489.51	19487.56
MNCL2	0.00	0.00	0.00	0.00	0.00	0.00	0.00	0.00	0.00	0.00
WATER	0.00	0.00	0.00	0.00	0.00	0.00	4000.00	5.00	5.00	0.00
C6H12	0.00	0.00	0.00	0.00	0.00	0.00	6000.00	3.00	3.00	0.00
Mn^{2+}	0.00	0.00	0.00	0.00	0.00	0.00	87.31	0.00	0.00	0.00
Cl^-	0.00	0.00	0.00	0.00	0.00	0.00	112.69	0.00	0.00	0.00

Table. S20. Mass balance of PET methanolysis in synergistic system (continued).

Stream	RC6H12	MIX	EGOUT	RCAT1	RDMT	RDMT1	RMEOH	RMHET	RMNCL
Temperature (℃)	86.2	25.0	198.2	180.0	290.3	30.0	63.7	336.5	86.2
Pressure (bar)	1.0	1.0	1.2	30.0	1.2	1.0	0.8	1.5	1.0
Mass flow (kg/hr)	5996.10	10000.00	5434.05	1800.00	19449.21	14868.61	294314.78	851.57	4202.99
PET	0.00	0.00	0.00	0.00	0.00	0.00	0.00	0.00	0.00
CH3OH	0.05	0.00	0.00	0.00	0.00	0.00	293427.78	0.00	5.80
MN2O3	0.00	0.00	0.00	1800.00	0.00	0.00	0.00	0.00	0.00
EG	0.05	0.00	5424.10	0.00	0.54	0.00	818.32	0.00	1.19
BHET	0.00	0.00	0.00	0.00	0.00	0.00	0.00	29.50	0.00
MHET	0.00	0.00	0.00	0.00	0.08	0.00	0.04	783.09	0.00
DMT	0.00	0.00	1.95	0.00	19448.59	14668.61	68.64	38.98	0.00
MNCL2	0.00	0.00	0.00	0.00	0.00	0.00	0.00	0.00	0.00
WATER	2.00	4000.00	5.00	0.00	0.00	0.00	0.00	0.00	3993.00
C6H12	5994.00	6000.00	3.00	0.00	0.00	0.00	0.00	0.00	3.00
Mn^{2+}	0.00	0.00	0.00	0.00	0.00	87.31	0.00	0.00	87.31
Cl^-	0.00	0.00	0.00	0.00	0.00	112.69	0.00	0.00	112.69

Table. S21. Mass balance of PET methanolysis in heterogeneous system.

Stream	PET	MEOH	CAT	0001	0002	0003	0004	0005	0006	0007
Temperature (℃)	25.0	25.0	25.0	25.0	180.0	180.0	180.0	30.0	30.0	70.0
Pressure (bar)	1.0	1.0	1.0	1.0	30.0	30.0	30.0	1.0	1.0	1.2
Mass flow (kg/hr)	20000.00	300000.00	2000.00	322000.00	322000.00	322000.00	301574.31	301574.31	300382.86	297968.55
PET	20000.00	0.00	0.00	20000.00	20000.00	18425.69	0.00	0.00	0.00	0.00
CH3OH	0.00	300000.00	0.00	300000.00	300000.00	299475.37	299475.37	299475.37	299475.37	297538.47
MN2O3	0.00	0.00	2000.00	2000.00	2000.00	2000.00	0.00	0.00	0.00	0.00
EG	0.00	0.00	0.00	0.00	0.00	507.77	507.77	507.77	507.77	419.53
BHET	0.00	0.00	0.00	0.00	0.00	0.00	0.00	0.00	0.00	0.00
MHET	0.00	0.00	0.00	0.00	0.00	2.57	2.57	2.57	2.57	0.00
DMT	0.00	0.00	0.00	0.00	0.00	1588.60	1588.60	1588.60	397.15	10.56

Table. S22. Mass balance of PET methanolysis in heterogeneous system (continued).

Stream	0008	0009	0010	0011	EGOUT	MEHTOUT	MEOH-REC	RCATPET	RDMT1	RDMT2
Temperature (℃)	70.0	58.6	182.7	305.1	146.9	343.8	65.0	180.0	30.0	294.0
Pressure (bar)	1.2	0.8	1.2	1.5	1.2	1.5	0.8	30.0	1.0	1.2
Mass flow (kg/hr)	2414.31	1933.12	481.19	389.13	92.06	3.34	299901.67	20425.69	1191.45	385.79
PET	0.00	0.00	0.00	0.00	0.00	0.00	0.00	18425.69	0.00	0.00
CH3OH	1936.90	1933.03	3.87	0.00	3.87	0.00	299471.50	0.00	0.00	0.00
MN2O3	0.00	0.00	0.00	0.00	0.00	0.00	0.00	2000.00	0.00	0.00
EG	88.24	0.09	88.15	0.01	88.14	0.00	419.62	0.00	0.00	0.01
BHET	0.00	0.00	0.00	0.00	0.00	0.00	0.00	0.00	0.00	0.00
MHET	2.57	0.00	2.57	2.57	0.00	2.57	0.00	0.00	0.00	0.00
DMT	386.59	0.00	386.59	386.55	0.04	0.77	10.56	0.00	1191.45	385.78

Table. S23. Comparison of economic balance.

Category	unit	Synergistic system	Heterogeneous system
Total Capital Cost	[USD/Year]	10895750	8302370
	[CNY/Year]	75616500	57618400
Total Operating Cost	[USD/Year]	1415787900	1300530000
	[CNY/Year]	9825568000	9025678200
Total Raw Materials Cost	[USD/Year]	1234100000	1182510000
	[CNY/Year]	8564654000	8206619400
Total Product Sales	[USD/Year]	1710640000	1217780000
	[CNY/Year]	11871841600	8451393200
Total Utilities Cost	[USD/Year]	21993500	19874900
	[CNY/Year]	152635100	137931800
Equipment Cost	[USD]	4433800	3792100
	[CNY]	30770500	26317100
Total Installed Cost	[USD]	7854100	6563600
	[CNY]	54507400	45551300
P.O. Period [Year]		5.8	Unprofitable

Note: This study evaluated the economic feasibility of the two processes using the built-in economic analysis module in Aspen Plus V14. The prices of raw materials and products were referenced from the published quotations of reagent suppliers such as Shanghai Aladdin and common market procurement prices, while the utility costs were based on the built-in energy prices of the software.

Table. S24. Comparison of electricity consumption.

	Name	Fluid	Rate	Cost per Hour [USD/H]	Cost per Hour [CNY/H]
Synergistic system	Electricity		201.52 [KW]	15.62	108.40
	Cooling Water	Water	1.23 [MMGAL/H]	147.96	1026.84
	Steam @165PSI	Steam	230.00 [KLB/H]	2244.77	15578.70
	Steam @400PSI	Steam	8.24 [KLB/H]	96.54	669.99
Heterogeneous system	Electricity		201.52 [KW]	15.62	108.40
	Cooling Water	Water	1.10 [MMGAL/H]	132.34	918.44
	Steam @165PSI	Steam	217.14 [KLB/H]	2119.32	14708.08

Table. S25. Details of tower equipment parameters.

	Item Description	TOWER3	TOWER2	TOWER1
Synergistic system	Diameter Bottom section [meter]	1.3716	0.6096	0.4572
	Bottom tangent to tangent height [meter]	29.8704	18.288	20.1168
	Design gauge pressure Bottom [barg]	2.434211	2.4342108	2.4342108
	Design temperature Bottom [℃]	330.0779	330.077925	236.4711078
	Operating temperature Bottom [℃]	302.3001	302.3001472	208.69333
	Number of trays Bottom section	43	24	27
	Bottom Tray type	SIEVE	SIEVE	SIEVE
	Bottom Tray spacing [meter]	0.6096	0.6096	0.6096
Heterogeneous system	Diameter Bottom section [meter]	0.4572	0.4572	0.4572
	Bottom tangent to tangent height [meter]	21.336	18.8976	32.9184
	Design gauge pressure Bottom [barg]	2.4342108	2.4342108	2.4342108
	Design temperature Bottom [℃]	371.5551	332.9184939	121.1111111
	Operating temperature Bottom [℃]	343.7773222	305.1407161	70
	Number of trays Bottom section	29	25	48
	Bottom Tray type	SIEVE	SIEVE	SIEVE
	Bottom Tray spacing [meter]	0.6096	0.6096	0.6096

Table. S26. Comparison of equipment installation cost.

	Operational Unit	Equipment Cost [USD]	Equipment Cost [CNY]	Installed Cost [USD]	Installed Cost [CNY]	Equipment Weight [LBS]	Installed Weight [LBS]	Utility Cost [USD/HR]	Utility Cost [CNY/HR]
Synergistic system	TOWER3	310600	2155564	672500	4667150	51000	97979	0	0
	FLASH1	435700	3023758	830600	5764364	114800	168007	0	0
	HEATER2	22800	158232	116800	810592	2700	15500	96.54	669.9876
	1-Sep	284100	1971654	554900	3851006	90000	132220	0	0
	TOWER2	114000	791160	333900	2317266	15300	37199	0	0
	COOLER1	1528200	10605708	2105000	14608700	289600	395664	147.96	1026.8424
	HEATER	666900	4628286	1043800	7243972	117800	187272	2244.77	15578.704
	TOWER1	124600	864724	337100	2339474	24000	42817	0	0
	3-Sep	26200	181828	173500	1204090	3100	15354	0	0
	REACTOR	776800	5390992	1108200	7690908	136300	179901	0	0
	2-Sep	118500	822390	388100	2693414	27200	55658	0	0
Heterogeneous system	TOWER3	152000	1054880	455800	3163252	29800	51853	0	0
	FLASH2	307500	2134050	691000	4795540	70900	122490	0	0
	COOLER1	970300	6733882	1382400	9593856	184600	256184	132.34	918.4396
	1-Sep	281500	1953610	551800	3829492	89000	131116	0	0
	TOWER2	101900	707186	319200	2215248	18700	39681	0	0
	FLASH1	118500	822390	388100	2693414	27200	55658	0	0
	HEATER1	634900	4406206	968100	6718614	111200	171055	2119.32	14708.081
	TOWER1	455600	3161864	706500	4903110	138500	159942	0	0
	REACTOR	769900	5343106	1100700	7638858	134900	178412	0	0

Table. S27. Details of heat exchanger parameters.

Item description	Synergistic system		Heterogeneous system		
	HEATER2	COOLER1	HEATER	COOLER1	HEATER1
Heat transfer area [sqm]	32.91	4180.43	2583.07	2656.12	2437.29
Tube design gauge pressure [barg]	30.01	21.29	12.09	21.29	12.09
Tube design temperature [°C]	257.00	207.78	212.00	207.78	212.00
Tube operating temperature [°C]	229.22	35.00	184.22	35.00	184.22
Tube outside diameter [meter]	0.03	0.03	0.03	0.03	0.03
Shell design gauge pressure [barg]	19.67	32.43	7.72	32.43	7.72
Shell design temperature [°C]	227.78	207.78	207.78	207.78	207.78
Shell operating temperature [°C]	200.00	180.00	180.00	180.00	180.00
Tube length extended [meter]	6.10	6.10	6.10	6.10	6.10
Tube pitch [meter]	0.03	0.03	0.03	0.03	0.03

Table. S28. Details of reactor parameters.

Item description	Synergistic system	Heterogeneous system
	REACTOR	**REACTOR**
Liquid volume [L]	57646.39	56745.67
Vessel diameter [meter]	2.74	2.74
Vessel tangent to tangent height [meter]	9.75	9.60
Design gauge pressure [barg]	32.43	32.43
Design temperature [°C]	207.78	207.78

Table. S29. Detailed utility parameters

Name	Type	Description
AIR	Common	Air, inlet temperature =30 ℃, outlet temperature =35 ℃
ELEC	Electricity	Electric utility engineering
LP	Steam	Low pressure steam, inlet temperature =125 ℃, outlet temperature ·=124 ℃
MP	Steam	Medium pressure steam, inlet temperature =175 ℃, outlet temperature =174 ℃, pressure =127 psi
OIL	Common	Hot oil, inlet temperature =280 ℃, outlet temperature =250 ℃
WATER	Water	Cooling water, inlet temperature =20 ℃, outlet temperature =25 ℃